Glutamic Acid Residues of Bacteriorhodopsin at the Extracellular Surface as Determinants for Conformation and Dynamics as Revealed by Site-Directed Solid-State ^{13}C NMR

Hazime Saitô,* Satoru Yamaguchi,* Keiji Ogawa,* Satoru Tuzi,* Mercedes Márquez,† Carolina Sanz,† and Esteve Padrós†

*Department of Life Science, Graduate School of Science, Himeji Institute of Technology, Harima Science Garden City, Kamgiori, Hyogo, Japan 678-1297; and †Unitat de Biofísica, Departament de Bioquímica i de Biologia Molecular, Facultat de Medicina, Universitat Autònoma de Barcelona, Bellaterra, Barcelona 08193, Spain

ABSTRACT We recorded ^{13}C NMR spectra of [3-^{13}C]Ala- and [1-^{13}C]Val-labeled bacteriorhodopsin (bR) and a variety of its mutants, E9Q, E74Q, E194Q/E204Q (2Glu), E9Q/E194Q/E204Q (3Glu), and E9Q/E74Q/E194Q/E204Q (4Glu), to clarify contributions of the extracellular (EC) Glu residues to the conformation and dynamics of bR. Replacement of Glu-9 or Glu-74 and Glu-194/204 at the EC surface by glutamine(s) induced significant conformational changes in the cytoplasmic (CP) surface structure. These changes occurred in the C-terminal α-helix and loops, and also those of the EC surface, as viewed from ^{13}C NMR spectra of [3-^{13}C]Ala- and [1-^{13}C]Val-labeled proteins. Additional conformational changes in the transmembrane α-helices were induced as modified retinal-protein interactions for multiple mutants involving the E194Q/E204Q pair. Significant dynamic changes were induced for the triple or quadruple mutants, as shown by broadened ^{13}C NMR peaks of [1-^{13}C]Val-labeled proteins. These changes were due to acquired global fluctuation motions of the order of 10^{-4}–10^{-5} s as a result of disorganized trimeric form. In such mutants ^{13}C NMR signals from Val residues of [1-^{13}C]Val-labeled triple and quadruple mutants near the CP and EC surfaces (including 8.7-Å depth from the surface) were substantially suppressed, as shown by comparative ^{13}C NMR studies with and without 40 μM Mn^{2+} ion. We conclude that these Glu residues at the EC surface play an important role in maintaining the native secondary structure of bR in the purple membrane.

INTRODUCTION

Bacteriorhodopsin (bR) is a light-driven proton pump, consisting of seven transmembrane α-helices containing a retinal molecule linked to Lys-216 through a protonated Schiff base, in the purple membrane of *Halobacterium salinarum*. Upon excitation with light, bR undergoes a cyclic photoreaction with intermediates, J, K, L, M, N, and O (Ovchinnikov, 1982; Stoeckenius and Bogomolni, 1982; Mathies et al., 1991; Lanyi, 1993, 1997). During the L-to-M transition, a proton is transferred from the protonated Schiff base to the proton acceptor Asp-85 and another proton is subsequently released on the extracellular (EC) side from the proton releasing complex (Glu-204, Glu-194, and a bound water). This can be seen in the primary sequence of bR by taking into account the secondary structure in Fig. 1 (Brown et al., 1995; Dioumaev et al., 1998; Luecke et al., 1998). The proton is taken up on the cytoplasmic (CP) surface through reprotonation of Asp-96 from the environment, after the Schiff base has been reprotonated by Asp-96 (Brown et al., 1994, 1995; Yamazaki et al., 1995, 1996; Balashov et al., 1997).

The presence of negatively charged amino-acid residues is associated with the binding site for protons and a variety of mono- or divalent cations. The presence of specific cation binding sites was initially proposed to explain the alterations of the color and the above-mentioned function of bR (Chang et al., 1985; Ariki and Lanyi, 1986). However, Szundi and Stoeckenius (1987, 1989) demonstrated that lowered surface pH, induced by removal of nonspecific surface-bound cations, can explain the purple-to-blue transition. In any case, the presence of negatively charged amino-acid residues such as Glu or Asp is primarily responsible for interaction with protons or cations located at the membrane surface, together with the negatively charged lipid molecules from *H. salinarum*. We have previously shown that the most preferred high-affinity cation binding site is located at the F-G loop near Ala-196 on the EC surface, as viewed by ^{13}C NMR (Tuzi et al., 1999). Besides, the negatively charged Glu residues located on the EC surface are also sites for bound divalent cations, essential for the stabilization of EC structure and proton pump activity (Sanz et al., 1999, 2001). Further, Lazarova et al. (2000) also suggested that Glu-194 controls the pK_a of Asp-85.

In contrast, Glu and Asp residues on the CP surface have been examined to clarify the proton uptake mechanism from the CP surface, leading to protonation at Asp-96. In particular, Asp-38 is an essential part of the proton translocation pathway in the late steps of the functional cycle, the modulation of the hydrogen-bond network, and the reprotonation of the Schiff base (Riesle et al., 1996). Further, Asp-36, Asp-38, Asp-102, Asp-104, and Glu-161 appear to efficiently collect protons from the aqueous bulk phase and channel them to the entrance of the CP proton pathway

Submitted June 19, 2003, and accepted for publication November 4, 2003.

Address reprint request to Dr. Hazime Saitô, Dept. of Life Science, Himeji Institute of Technology, Harima Science Garden City, Kouto 3-chome, Kamigori, Hyogo 678-1297, Japan. Tel./Fax: +81-78-856-2876; E-mail: saito@sci.himeji-tech.ac.jp.

0006-3495/04/03/1673/09 $2.00

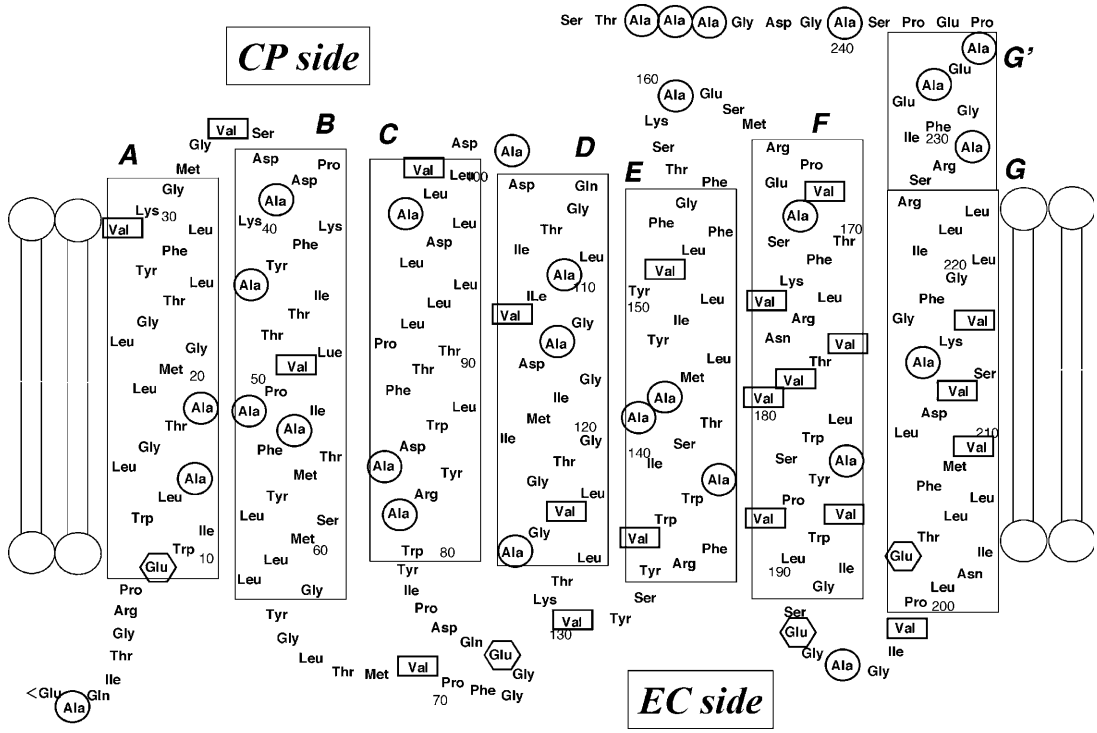

FIGURE 1 Schematic representation of the primary sequence of bacteriorhodopsin, taking into account the secondary structure obtained by x-ray diffraction studies (Luecke et al., 1998). The [3-^{13}C]Ala- and [1-^{13}C]Val-labeled residues are shown as circled and boxed residues, respectively. The extracellular Glu residues are marked by hexagons.

(Riesle et al., 1996; Checover et al., 1997, 2001). Brown et al. (1999), however, showed that only Asp-36 could play a direct role in proton uptake at the CP surface. On the basis of site-directed ^{13}C NMR studies on bR and a variety of mutants, it was demonstrated that the cytoplasmic surface complex consisting of the α-helix protruding from the membrane surface and CP-loops through salt bridge and/or metal ion-mediated interactions is strongly related with efficient proton uptake. This is done through suppression of motional fluctuations at the region of the proton collecting antenna (Yonebayashi et al., 2003).

In particular, we have recently demonstrated that the study of [3-^{13}C]Ala- or [1-^{13}C]Val-labeled membrane proteins by ^{13}C NMR provides an effective means of examining the local conformation and dynamics in a site-specific manner as recorded by cross-polarization-magic angle spinning (CP-MAS) and single-pulse dipolar decoupled-magic angle spinning (DD-MAS) NMR. This approach takes advantage of the assigned ^{13}C chemical shifts of a variety of residues in [3-^{13}C]Ala- and [1-^{13}C]Val-labeled bR (Table 1). The information is based on the data of the conformation-dependent displacements of ^{13}C chemical shifts from model polypeptides, and comparison of the peak intensities of a variety of site-directed mutants with those of wild type, enzymatic cleavage, etc. (Saitô, 1986; Saitô and Ando, 1989; Saitô et al., 1998, 2000, 2002a,c). It is also emphasized that ^{13}C CP-MAS NMR signals from the N- or C-terminal portions of [3-^{13}C]Ala-bR undergoing flexible fluctuation motions with correlation times shorter than 10^{-8} s are virtually suppressed owing to time-averaged ^{13}C-^{1}H dipolar interactions. However, ^{13}C signals from whole areas are recorded by DD-MAS NMR as far as their ^{13}C spin-lattice relaxation times are sufficiently shorter ($\sim$0.5 s in the case of Ala C_β; Tuzi et al., 1996) than the repetition time (6 s) for spectral acquisition. Therefore, ^{13}C NMR signals from such flexible regions can be distinguished from those of other regions by combined use of these ^{13}C NMR techniques. In addition, local fluctuation motions with correlation times of the order of 10^{-4} or 10^{-5} s can be readily distinguished through identification of suppressed ^{13}C NMR peaks in both the CP-MAS and DD-MAS measurements. This is based on the failure of attempted peak-narrowing process, as high-resolution solid-state NMR interfered with the frequency of either magic angle spinning or proton decoupling, respectively (Suwelack et al., 1980; Rothwell and Waugh, 1981; Saitô et al., 2000, 2002a). The ^{13}C NMR approach has been applied successfully to the analysis of other membrane proteins that are recalcitrant to other methods, such as diffraction due to fluctuation motions.

In this study we recorded ^{13}C CP- and DD-MAS NMR spectra of [3-^{13}C]Ala or [1-^{13}C]Val-labeled bR (see the *circled* and *boxed residues*, respectively, in Fig. 1), and its single and multiple mutants in which extracellular Glu residues (marked by the *hexagons*) were replaced with Gln.

TABLE 1 Assigned ^{13}C chemical shifts for [3-^{13}C]Ala- and [1-^{13}C]Val-labeled bacteriorhodopsin (ppm from TMS)

		Ala	Val
[3-^{13}C]Ala*	17.78	196	
	17.36	160	
	17.27	184	
	17.19	103, 235	
	16.88	84, 240, 244–246	
	16.38	39, 168	
	16.52	81	
	16.20	215	
	16.14	53	
	15.92	51	
	15.91–15.67	228, 233	
	15.38	126	
[1-^{13}C]Val†	171.07		101, 199
	171.99		49, 130
	172.84		34, 69
	173.97		151, 167, 180
	174.60		136, 179, 187
	174.97		217
	177.04		29, 213

*Taken from Yamaguchi et al. (2001).
†Taken from Saitô et al. (2004).

We aimed to clarify the structural role of Glu residues located at the EC surface for structural and dynamics aspect of EC as well CP surfaces.

MATERIALS AND METHODS

L-[3-^{13}C]Ala and L-[1-^{13}C]Val were purchased from CIL (Andover, MA) and used without purification. The bR mutants, E9Q, E74Q, E194Q/E204Q (2Glu), E9Q/E194Q/E204Q (3Glu), and E9Q/E74Q/E194Q/E204Q (4Glu) were prepared as described (Sanz et al., 1999). They were grown in temporary synthetic (TS) medium of Onishi et al. (1965), in which unlabeled L-alanine or L-valine was replaced by L-[3-^{13}C]Ala or L-[1-^{13}C]Val, respectively. The bR preparations containing 10 mM NaCl, 5 mM HEPES buffer (pH 7), and 0.025% (w/v) NaN_3 from these sources were isolated by the method of Oesterhelt and Stoeckenius (1974). Mn^{2+} treatment of these preparations was carried out by resuspension of the purple membrane twice in 5 mM HEPES buffer (pH 7) containing 10 mM NaCl, 0.025% NaN_3, and 40 μM Mn^{2+} to adjust the final absorbance to 1.0. The samples thus prepared were concentrated by centrifugation. The pelleted preparations (~10 mg protein) thus obtained were placed into a 5-mm OD zirconium pencil-type rotor. The caps were tightly glued to the rotor by rapid Alardite (Vantico, East Lansing, MI) to prevent leakage of water from the samples during magic angle spinning under a stream of dried air. All samples for NMR measurements were placed in the dark before measurement, for at least 2 days at 23°C.

High-resolution ^{13}C NMR spectra (100.6 MHz) were recorded in the dark at 20°C on a Chemagnetics (Fort Collins, CO) CMX-400 NMR spectrometer by cross-polarization-magic angle spinning with total suppression of spinning sidebands (TOSS). The spectral width, contact, acquisition, and repetition times were 40 kHz, 1 ms, 50 ms, and 4 s, respectively. The $\pi/2$ pulses for carbon and proton nuclei were 5 μs and the spinning rate was 4 kHz. The $\pi/4$ pulse for carbon was used to acquire single pulse DD-MAS NMR spectra with a repetition time of 6 s. Free induction decays were acquired with data points of 2 K and accumulated 6000 ~ 20,000 times depending upon their signal/noise ratios. Fourier transforms were carried out as 16-K data points after 14-K data points were zero-filled. Resolution was enhanced by Gaussian multiplication (Gaussian broadening and Lorentzian broadening were 30 and 10 Hz, respectively). ^{13}C chemical shifts were first referred to the carboxyl signal of glycine (176.03 ppm from tetramethylsilane (TMS)) and then expressed as relative shifts from the value of TMS.

RESULTS

Fig. 2 compares the ^{13}C CP-MAS (*left*) and DD-MAS (*right*) NMR spectra of [3-^{13}C]Ala-labeled E9Q (*C* and *D*) and E74Q mutants (*E* and *F*) with those of wild type (*A* and *B*). The loop region of the CP surface consisting of the C-terminal α-helix complexed with the C-D and E-F loops (Yamaguchi et al., 2001b; Yonebayashi et al., 2003) resonated at 17.0–17.8 ppm, was altered by these single mutations at the EC surface. In particular, the ^{13}C NMR signal of Ala-103 from the C-D loop of these mutants is displaced downfield to 17.55 ppm from 17.20 ppm wild type. Further, the ^{13}C NMR peaks of Ala-228 and Ala-233 from the C-terminal α-helix are displaced upfield from 15.91 to 15.82 ppm, respectively, as a result of the modified CP surface structure. Similar spectral changes were also seen for A168G and E166G (E-F loop) and R227Q mutants (C-terminal α-helix) (Yonebayashi et al., 2003) at the proton collecting antenna (Checover et al., 1997). In addition, the increased peak-intensities of the lowest peak at 19.83 ppm of E74Q and E9Q mutants, ascribed to lipid methyl group (Tuzi et al., 1993), are caused, presumably, by an increased number of surrounding lipid molecules or by an altered lipid content, due to the presence of a disorganized trimeric structure (Saitô et al., 2002b).

Such a local conformational change, due to a single mutation such as E9Q or E74Q, appears mainly localized at the EC and CP surface areas, because the observed ^{13}C NMR spectral change of [1-^{13}C]Val-labeled protein is restricted to DD-MAS NMR spectra alone (Fig. 3, *right*). Actually, no distinct spectral change was noted from the ^{13}C CP-MAS NMR spectra sensitive to the conformation and dynamics of the transmembrane α-helices (Fig. 3, *left*) among bR, E9Q, and E74Q mutants. To substantiate this, it should be noted that distinct dynamic changes at the EC and CP surfaces produce partially suppressed peaks at 171.0 ppm (Val-199 and Val-101) and 172.0 ppm (Val-130) (Saitô et al., 2002c, 2003a).

Fig. 4 illustrates the ^{13}C CP-MAS (*left*) and DD-MAS (*right*) NMR spectra of [3-^{13}C]Ala-labeled 2Glu (*C* and *D*), 3Glu (*E* and *F*), and 4Glu (*G* and *H*) mutants, as well as those of wild type (*A* and *B*), respectively. The resulting spectral lines from whole areas of these mutants were significantly broadened, as compared with those of wild type, owing to partially failed proton decoupling interfering with the fluctuation frequency in the order of 10^5 Hz (Rothwell and Waugh, 1981). As a result, the three well-resolved upper field peaks at 15.34, 15.02, and 14.74 ppm of wild type (see Fig. 1 *A*) are no longer resolved for these multiple mutants. In contrast the corresponding peaks at 15.02 and 14.74 ppm are well resolved for both E194Q and E204Q single mutants

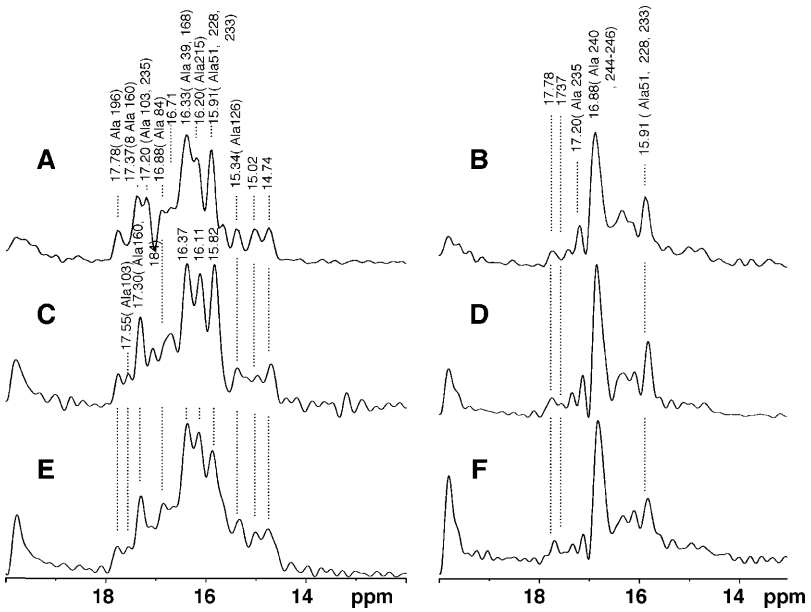

FIGURE 2 ^{13}C CP-MAS (*left*) and DD-MAS (*right*) NMR spectra of [3-^{13}C]Ala-labeled wild-type (*A* and *B*), E9Q (*C* and *D*), and E74Q (*E* and *F*) mutants. The assigned peaks, so far performed, are indicated at the top of the traces.

(Tanio et al., 1999). In addition, the increased peak-intensities at 19.83 ppm from the lipid methyl group of 3Glu and 4Glu as recorded by the DD-MAS spectra are interpreted in terms of increased numbers of surrounding lipids, as described above for the E9Q and E74Q mutants.

Therefore, the multiple mutants containing at least both E194Q and E204Q cause a retinal-protein perturbation that is not seen in the individual single mutants. This perturbation is consistent with the altered absorbance spectrum described for the 4Glu mutant that, at low ionic strength and neutral or alkaline pH, shows a λ_{max} of ~515 nm (Sanz et al., 1999). In addition, the ^{13}C NMR signals resonated at 17.78 (Ala-196 from the F-G loop) and 15.91 ppm (Ala-228 and Ala-233 at the C-terminal α-helix) of these mutants are appreciably suppressed as compared to those of wild type in the CP-MAS NMR only, but the peak at 16.33 (Ala-39 and Ala-168) and 16.20 ppm (Ala-15) (both at the CP ends of B and F helices, respectively) are suppressed for both the CP-MAS and DD-MAS NMR spectra. The former type of suppression arises from insufficient magnetization based on cross-polarization from nearby protons due to the presence of time-averaged dipolar interactions with correlation times shorter than 10^{-8} s, whereas the latter type of suppression is caused by interference of incoherent motional frequency (in the order of 10^{-5} s) with the coherent frequency of proton decoupling (Rothwell and Waugh, 1981; Saitô et al., 2000).

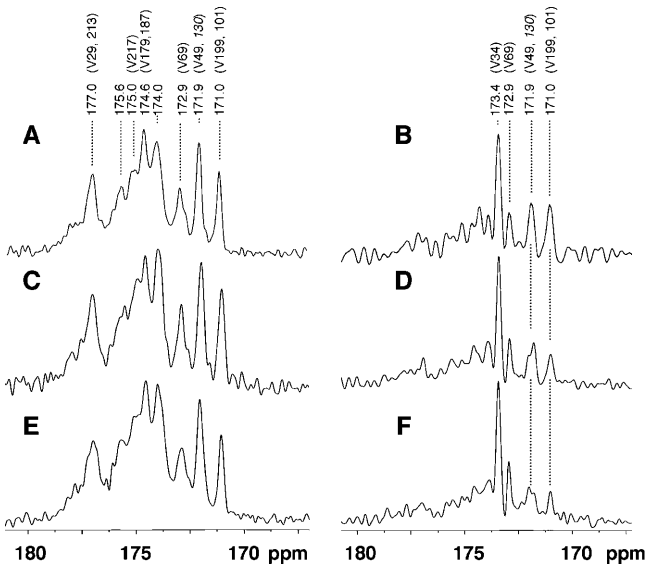

FIGURE 3 ^{13}C CP-MAS (*left*) and DD-MAS (*right*) NMR spectra of [1-^{13}C]Val-labeled wild-type (*A* and *B*), E9Q (*C* and *D*), and E74Q (*E* and *F*) mutants. The assigned peaks, so far performed, are indicated at the top of the traces.

This timescale was estimated by the behavior of the suppressed ^{13}C NMR peaks for [3-^{13}C]Ala-labeled mutants as compared to those for wild-type bR. In particular, the presence of rapid isotropic motions with timescale of $<10^{-8}$ s in the C-terminal end can be detected by selectively suppressed peaks in the CP-MAS experiment as compared with those in the DD-MAS experiment. This is due to the presence of motionally averaged dipolar interaction with this timescale, which results in selective suppression of the peaks recorded by the CP-MAS experiment (Saitô et al., 2000, 2002a). In contrast, anisotropic conformational fluctuation of slow motions with correlation time of the order of 10^{-4} or 10^{-5} s could be readily distinguished by examination of either broadened or suppressed peaks from the [3-^{13}C]Ala-labeled proteins as well as [1-^{13}C]Val-labeled ones, as described below, respectively, because incoherent fluctuational frequencies of these motions are interfered by coherent frequencies of the dipolar decoupling or magic angle

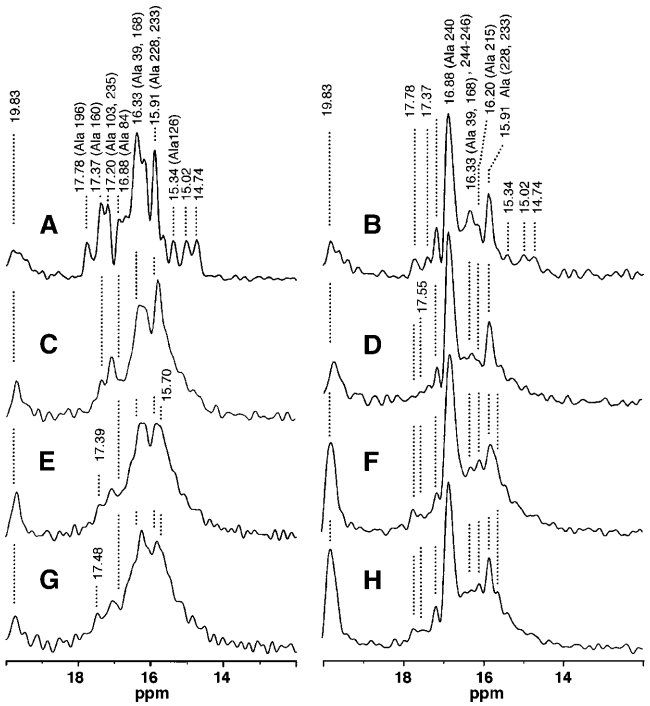

FIGURE 4 ^{13}C CP-MAS (*left*) and DD-MAS (*right*) NMR spectra of [3-^{13}C]Ala-labeled wild-type (*A* and *B*), E194Q/E204Q (2Glu) (*C* and *D*), E9Q/E194Q/E204Q (3Glu) (*E* and *F*), and E9Q/E74Q/E194Q/E204Q (4 Glu) (*G* and *H*) mutants. The assigned peaks, so far performed, are indicated at the top of the traces.

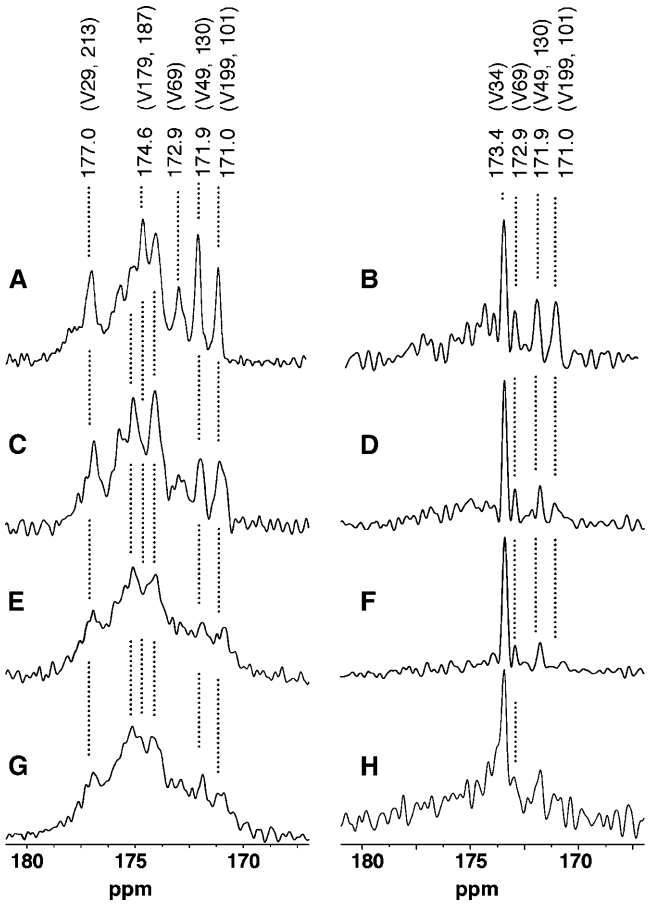

FIGURE 5 ^{13}C CP-MAS (*left*) and DD-MAS (*right*) NMR spectra of [1-^{13}C]Val-labeled wild-type (*A* and *B*), E194Q/E204Q (2Glu; *C* and *D*), E9Q/E194Q/E204Q (3Glu; *E* and *F*), and E9Q/E74Q/E194Q/E204Q (4 Glu; *G* and *H*) mutants.

spinning, respectively (Suwelack et al., 1980; Rothwell and Waugh, 1981). In such cases, resulting failure of the peak-narrowing process to achieve high-resolution NMR permits the estimation of the timescale of such slow motions (Saitô et al., 2000, 2002a).

Fig. 5 shows the ^{13}C CP-MAS (*left*) and DD-MAS (*right*) NMR spectra of [1-^{13}C]Val-labeled 2Glu (*C* and *D*), 3Glu (*E* and *F*), and 4Glu (*G* and *H*), with reference to those of wild type (*A* and *B*). The following spectral changes are noteworthy: First, the peak at 174.6 ppm of wild type ascribable to Val-179 and Val-187 (Saitô et al., 2004) was displaced downfield to 175.0 ppm for the multiple mutants involving E194Q/E204Q. This kind of spectral change was also noted for D85N (Kawase et al., 2000) and bO (Yamaguchi et al., 2001a), as a characteristic peak arising from modified retinal/protein interactions. It is also significant that a similar spectral change was noted for [1-^{13}C]Val-bR reconstituted into the lipid bilayers (Saitô et al., 2003) in which the trimeric structure is no longer retained (Dencher et al., 1983). More drastic dynamics changes were noteworthy for the triple and quadruple mutants, however, as manifested by the substantially broadened ^{13}C NMR signals of [1-^{13}C]Val-labeled proteins due to acquired global fluctuation motions for whole proteins of the order of 10^{-4}–10^{-5} s.

Fig. 6 compares the ^{13}C CP-MAS NMR signals of [1-^{13}C]Val-labeled wild type (*A*), 3Glu (*B*), and 4Glu (*C*) with (*solid lines*) and without (*dotted lines*) 40-μM Mn^{2+} ion, to clarify to what extent ^{13}C NMR signals from the surface areas are visible or suppressed in the presence of the Mn^{2+} ion. This is because ^{13}C NMR signals from residues located at the membrane surface areas are suppressed by accelerated transverse relaxation times from surface-bound Mn^{2+} ions. The magnitude of the dipole-dipole interaction between the electron spin of Mn^{2+} ion and the ^{13}C nucleus is expressed as a function of the distance between the electron spin from the Mn^{2+} ion and the ^{13}C nuclei, and the correlation time of rotational reorientation of the spin pair, according to Solomon-Bloembergen Eq. 1 (Solomon, 1955; Bloembergen, 1957),

$$1/T_{2c} = [S(S+1)\gamma_c^2 g^2 \beta^2]/15r^6][4\tau_{c1} + 3\tau_{c1}/(1+\omega_c^2\tau_{c1}^2) + 13\tau_{c2}(1+\omega_e^2\tau_{c2}^2)] \quad (1)$$

$$1/\tau_{c1} = 1/T_{1e} + 1/\tau_r + 1/\tau_m,$$

$$1/\tau_{c2} = 1/T_{2e} + 1/\tau_r + 1/\tau_m,$$

where T_{2c} is the spin-spin relaxation time of a ^{13}C nucleus,

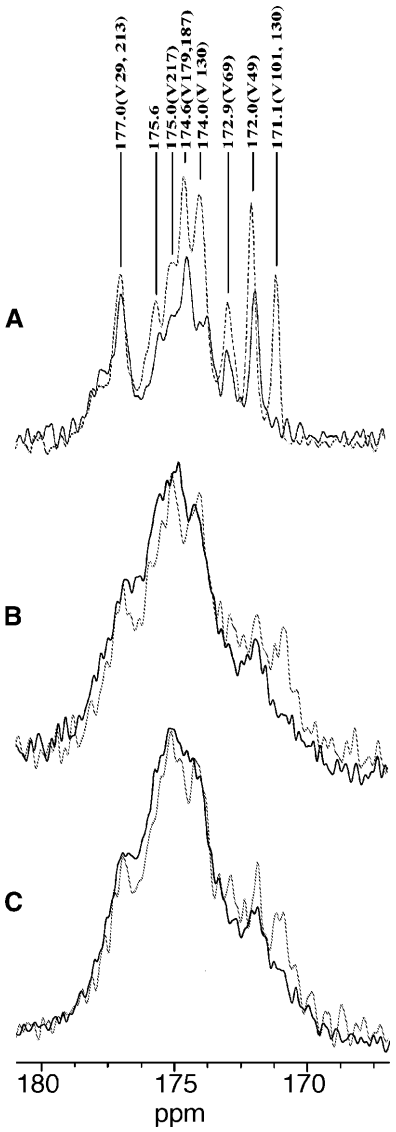

FIGURE 6 ^{13}C CP-MAS NMR spectra of [1-^{13}C]Val-labeled wild-type (*A*), E9Q/E194Q/E204Q (3Glu; *B*), and E9Q/E74Q/E194Q/E204Q (4 Glu; *C*) with (*solid lines*) and without (*dotted lines*) 40 μM Mn^{2+} ions.

r is the distance between the ^{13}C nucleus and Mn^{2+} ion, S is the total electron spin, ω_c and ω_e are the nuclear and electronic Larmor precession frequencies, γ_c is the gyromagnetic ratio of ^{13}C, g is the g-factor of Mn^{2+}, β is the Bohr magneton, T_{1e} and T_{2e} are the spin-lattice and spin-spin relaxation times of an electron, τ_r is the rotational correlation time of the Mn^{2+}-bR complex, and τ_m is the lifetime of the Mn^{2+} complex. The g-factor and T_{1e} of Mn^{2+} are assumed to be identical to those of an aqua ion. τ_m is assumed to be longer than T_{1e} (3×10^{-9} s). When τ_r is longer than T_{1e}, the line width corresponding to the calculated T_{2c} value becomes greater than 100 Hz in the area within 8.7 Å of Mn^{2+} ion (Tuzi et al., 2001, 2003).

Accordingly, it was expected that the presence of 40 μM Mn^{2+} ion could cause the suppression of the ^{13}C NMR signals of the residues located within 8.7-Å depth from the surface. However, the observed spectral patterns for [1-^{13}C]Val-labeled mutants were practically unchanged, despite the presence (*solid trace*) or absence (*dotted trace*) of Mn^{2+} ion (Fig. 6, *B* and *C*). This is because ^{13}C NMR spectra of [1-^{13}C]Val-labeled 3Glu and 4Glu, especially from the residues located at the surface and interfacial regions of the transmembrane α-helices, are appreciably suppressed by fluctuation motions coupled with frequency of magic angle spinning (Suwelack et al., 1980). Therefore, no signal from surface areas was left to be suppressed by the accelerated relaxation process in the presence of 40 μM Mn^{2+} ion. This finding indicates that the CP ends of the transmembrane α-helices and the EC loops acquire conformational flexibility of the order of 10^{-4} s in the multiple mutants, although no such motion is present in the wild type (Saitô et al., 2002b,c).

DISCUSSION

Modified CP surface structure by mutations of Glu-9 and Glu-74 residues at the EC surface

Single mutations of Glu residues such as Glu-9 or Glu-74 at the EC surface (see Fig. 1 for their locations) resulted in modified CP surface structure, as manifested by the specific displacements of ^{13}C NMR peaks from [3-^{13}C]Ala-labeled Ala-103 (C-D loop) and Ala-160 (E-F loop) residues in these proteins (Yamaguchi et al., 2001b; Yonebayashi et al., 2003) with respect to those of wild type, as demonstrated in Fig. 2. However, the resulting spectral changes in these single mutants are much smaller than those published for the single E194Q and E204Q mutants (Tanio et al., 1999). In fact, there appears to be no significant spectral change in Ala-196 (F-G loop) and Ala-126 (helix D) signals of E9Q or E74Q mutants, in contrast to the cases of E194Q and E204Q. This means that Glu-194 and/or Glu-204 at the proton-releasing group play a more essential role in the assembly of the tertiary structure of bR than Glu-9 and Glu-74.

The above-mentioned spectral change, therefore, seems to arise mainly from the modified structure of the CP surface consisting of the C-terminal α-helix, A-B, C-D, and E-F loops through salt bridges and/or metal-ion mediated linkages (Yonebayashi et al., 2003; Yamaguchi et al., 2001b). Therefore, a similar type of spectral change could be induced by single mutations at the E-F loop or its vicinity, such as E166G, A168G, or R227Q, which would perturb this surface structure (Yonebayashi et al., 2003). The former structural change, however, turned out to be restricted to the CP surface areas only, including the C-terminal tail and loops, since no significant change was induced in the conformation and dynamics in the transmembrane α-helices or the EC loops, as viewed from the comparison of the ^{13}C CP-MAS NMR spectral changes between [1-^{13}C]Val-labeled wild-type, E9Q, and E74Q mutants (Fig. 3).

This means that a long-distance transmission of the induced conformational or dynamics change from one side to the other may also occur in the opposite direction: mutation of a residue on one side such as E9Q or E74Q in the EC loops (Fig. 1) or A160G or A160V in the CP surface (Yamaguchi et al., 2001b) results in the conformational and dynamics changes on the other, as manifested from their respective ^{13}C NMR spectral changes. This kind of structural change could be directly transmitted from one side to the other through conformational and/or dynamics change(s) of amino-acid residues located at the loop regions serving as hinges, even if no conformational changes in the transmembrane α-helices themselves were directly involved, as in this situation. It is pointed out here that this kind of conformational and dynamics changes of amino-acid residues in the loops and also transmembrane α-helices might mediate signal transduction.

Glu residues as determinants of secondary structures of bR

As shown in Figs. 4 and 5, major conformational changes were induced when at least the two sites, Glu-194 and Glu-204 (see Fig. 1), were simultaneously mutated, as seen from the displaced ^{13}C NMR peaks of [3-^{13}C]Ala- or [1-^{13}C]Val-labeled proteins, in comparison with the single mutants (Tanio et al., 1999). As pointed out above, retinal-protein interactions are modified by the mutations involving Glu-194 and Glu-204 (Brown et al., 1995; Dioumaev et al., 1998; Luecke et al., 1998; Sanz et al., 1999). It is also interesting to note from Figs. 4 and 5 that the major dynamics change was favored by the presence of additional mutations at Glu-9 or at both Glu-9 and Glu-74, to result in a protein (the 3Glu or the 4Glu mutant) that differed from the wild type. Thus, in the 3Glu and 4Glu mutants, several Ala and Val residues located at the transmembrane α-helices and loops acquired different levels of motional flexibility, depending upon their specific locations, such as the C-terminal end (correlation time $< 10^{-8}$ s), cytoplasmic terminal ends of F and G helices (10^{-5} s; as viewed from the ^{13}C NMR spectra of [3-^{13}C]Ala-proteins), and transmembrane α-helices near to the ionone ring (10^{-4} s; as viewed from the ^{13}C NMR spectra of [1-^{13}C]Val-proteins).

It is interesting to note that the extent of acquired protein dynamics in these mutants is much greater than that of D85N at pH 10, taking an M-like state that is caused by relaxed retinal-protein interaction (Kawase et al., 2000). This sort of acquired flexibility of the protein backbone may be caused by both the disappearance of some interhelical interactions and the presence of extra space created by either the disrupted or the disorganized hexagonally packed lattice structure. The dynamic changes and the ensuing increased fluctuation motions detected in the multiple extracellular Glu mutants are in keeping with important structural and functional properties of these mutants (Sanz et al., 1999, 2001). On the one hand, differential scanning calorimetry (DSC) thermogram of wild-type bR shows two transitions. The main transition at ~98°C is due to the destruction of the helical interactions within the protein and retinal release, and a reversible pretransition at 80°C results from the disorganization of the hexagonal lattice. DSC measurements of these multiple mutants revealed a lack of the pretransition and a decrease in the temperature of the main transition (Sanz et al., 2001). This finding is consistent with the increased number of surrounding lipids, as shown by the increased peak intensities of the lipid methyl group at 19.83 ppm in the ^{13}C NMR spectra of [3-^{13}C]Ala-labeled mutants recorded by the DD-MAS NMR technique. Similar types of increased lipid molecules per protein were noted for other bR proteins: D85N (Kawase et al., 2000) in which the retinal-protein interactions were modified in the absence of electric charge at Asp-85, bacterioopsin from retinal deficient strain (Yamaguchi et al., 2000), or for W80L and W12L mutants due to disrupted or disorganized lattice structure (Saitô et al., 2002b). In addition, the decrease in the temperature of the main transition agrees with the mobility increase in these mutants.

On the other hand, these multiple mutated proteins reveal high accessibility of the solvent molecules to the protein interior, as detected by the high dependency of their absorption spectrum on changes in pH or ionic strength and by the rapid bleaching effect of hydroxylamine in the dark as well as in light (Sanz et al., 1999, 2001). This is consistent with the increased flexibility of the protein backbone, as detected by ^{13}C NMR spectral changes. The 4Glu mutant also showed decreased efficiency in M formation and proton transport (Sanz et al., 1999) that could be attributed to a back reaction to the BR resting state from an intermediate before M. A plausible explanation is that the rigidity of the protein needed to hold up the strain of the intermediate states is decreased due to increased flexibility.

Here, it should be taken into account that the ^{13}C NMR signals of [3-^{13}C]Ala- and [1-^{13}C]Val-labeled wild-type bR are fully visible (Figs. 2–6 and Saitô et al., 2004), but those signals from the multiple mutants are partially suppressed due to acquired fluctuation motions with the timescale of 10^{-4} s. To clarify whether the signals from the residues located at the surface were totally or partially suppressed, we compared the ^{13}C NMR spectra of [1-^{13}C]Val-bR with and without Mn^{2+} ion. The observed ^{13}C NMR peak intensity of [1-^{13}C]Val-bR of wild type turned out to be 41% in the presence of 40 μM Mn^{2+} ion, compared to that in the absence of Mn^{2+} ion (Fig. 6 *A*). This is consistent with the relative proportion of Val residues (38%) located at the membrane surface (8.7 Å from the negatively charged amino-acid residues) (Tuzi et al., 1999, 2003; Saitô et al., 2004). In contrast, ^{13}C NMR signals of the surface area of 3Glu and 4Glu were hardly affected by the presence of Mn^{2+}, indicating that the residues at the surface have already acquired conformational flexibility of the order of 10^{-4} s.

Another important consequence of the multiple Glu mutation is the impairment of the proposed cation binding sites in the extracellular region. It was shown that Ca^{2+}/bR values needed to restore 50% of the purple form from a deionized sample at pH 5, on the basis of calcium titration to deionized bR, are substantially increased from 2.1 for the wild type to 3.5, 8.0, and >10 for 2Glu, 3Glu, and 4Glu, respectively (Sanz et al., 2001). Further, Sanz et al. (2001) proposed two cation binding sites in the EC region of bR, having as ligands Glu-9, Glu-194, Glu-204, and water molecules. The most preferred cation binding site for divalent cations, as viewed from the site-directed ^{13}C NMR approach, is located at the F-G loop near Ala-196 close to this site, (Tuzi et al., 1999) and also at the CP site. The precise location of this site cannot be determined because of the fast chemical exchange process between various sites. Cation-binding site(s) near the membrane surface was proposed by Fu et al. (1997), and a site involving Glu-204 was anticipated because of theoretical calculation (Kusnetzow et al., 1999). Furthermore, a cation site located at less than 9.8 Å from Glu-74 was also proposed (Eliash et al., 2001). In any case, the most preferred site is located at the EC site and plays an essential role in maintaining the tertiary structure of bR.

This study provides an insight into the role of the EC Glu residues, mainly from the viewpoint of their degree of mobility. Although the single mutation of Glu-194 or Glu-204 disables the normal proton release process, this is not sufficient to destabilize the EC region, according to the ^{13}C NMR results. A substantial increase in mobility in this region is observed only when Glu-194 and Glu-204 are mutated simultaneously. When Glu-9 and/or Glu-74 are also mutated, the ^{13}C NMR results show that the mobility increases further, giving rise to a severely disorganized region. All previous indirect results are in keeping with an increase in mobility for these mutants, namely decreased thermal stability, decreased cation affinity, increase in the accessibility of the Schiff base environment, and other properties. Therefore, besides the involvement of Glu-194 and Glu-204 in proton release, the EC Glu residues can be considered as determinants of the bR structure.

We are indebted to one of the reviewers who suggested various ways to improve the correlation of the data reported.

This work was supported, in part, by a Grant-in-Aid for Scientific Research from the Ministry of Education, Culture, Sports, Science and Technology, Japan, and a BMC2000-0121 grant from the Dirección General de Investigación, Spain.

REFERENCES

Ariki, M., and J. K. Lanyi. 1986. Characterization of metal ion-binding sites in bacteriorhodopsin. *J. Biol. Chem.* 261:8167–8174.

Balashov, S. P., E. S. Imasheva, T. G. Ebrey, N. Chen, D. R. Menick, and R. K. Crouch. 1997. Glutamate-194 to cysteine mutation inhibits fast light-induced proton release in bacteriorhodopsin. *Biochemistry.* 36:8671–8676.

Bloembergen, N. 1957. Proton relaxation times in paramagnetic solutions. *J. Chem. Phys.* 27:572–573.

Brown, L. S., Y. Gat, M. Sheves, Y. Yamazaki, A. Maeda, R. Needleman, and J. K. Lanyi. 1994. The retinal Schiff base-counterion complex of bacteriorhodopsin: changed geometry during the photocycle is a cause of proton transfer to aspartate 85. *Biochemistry.*33:12001–12011.

Brown, L. S., R. Needleman, and J. K. Lanyi. 1999. Functional roles of aspartic acid residues at the cytoplasmic surface of bacteriorhodopsin. *Biochemistry.* 38:6855–6861.

Brown, L. S., J. Sasaki, H. Kandori, A. Maeda, R. Needleman, and J. K. Lanyi. 1995. Glutamic acid 204 is the terminal proton release group at the extracellular surface of bacteriorhodopsin. *J. Biol. Chem.* 270:27122–27126.

Chang, C. H., J. G. Chen, R. Govindjee, and T. Ebrey. 1985. Cation binding by bacteriorhodopsin. *Proc. Natl. Acad. Sci. USA.* 82:396–400.

Checover, S., Y. Marantz, E. Nachliel, M. Gutman, M. Pfeffer, J. Tittor, D. Oesterhelt, and N. A. Dencher. 2001. Dynamics of the proton transfer reaction on the cytoplasmic surface of bacteriorhodopsin. *Biochemistry.* 40:4281–4292.

Checover, S., E. Nachliel, N. A. Dencher, and M. Gutman. 1997. Mechanism of proton entry into the cytoplasmic section of the proton-conducting channel of bacteriorhodopsin. *Biochemistry.* 40:4281–4292.

Dencher, N. A., K.-D. Kohl, and M. P. Heyn. 1983. Photochemical cycle and light-dark adaptation of monomeric and aggregated bacteriorhodopsin in various lipid environments. *Biochemistry.* 22:1323–1334.

Dioumaev, A. K., H. T. Richter, L. S. Brown, M. Tanio, S. Tuzi, H. Saitô, Y. Kimura, R. Needleman, and J. K. Lanyi. 1998. Existence of a proton transfer chain in bacteriorhodopsin: participation of Glu-194 in the release of protons to the extracellular surface. *Biochemistry.* 37:2496–2506.

Eliash, T., L. Weiner, M. Ottolenghi, and M. Sheves. 2001. Specific binding sites for cations in bacteriorhodopsin. *Biophys. J.* 81:1155–1162.

Fu, X., M. Blesser, M. Ottoleghi, T. Eliash, N. Friedman, and M. Sheves. 1997. Titration kinetics of Asp-85 in bacteriorhodopsin: exclusion of the retinal pocket as the color-controlling cation binding site. *FEBS Lett.* 416:167–170.

Kawase, Y., M. Tanio, A. Kira, S. Yamaguchi, S. Tuzi, A. Naito, M. Kataoka, J. K. Lanyi, R. Needleman, and H. Saito. 2000. Alteration of conformation and dynamics of bacteriorhodopsin induced by protonation of Asp85 and deprotonation of Schiff base as studied by ^{13}C NMR. *Biochemistry.* 39:14472–14480.

Kusnetzow, A., D. L. Singh, C. H. Martin, I. L. Barani, and R. R. Birge. 1999. Nature of chromophore binding site of bacteriorhodopsin: the potential role of Arg82 as a principal counterion. *Biophys. J.* 76:2370–2389.

Lanyi, J. K. 1993. Proton translocation mechanism and energetics in the light-driven pump bacteriorhodopsin. *Biochim. Biophys. Acta.* 1183: 241–261.

Lanyi, J. K. 1997. Mechanism of ion transport across membranes. bacteriorhodopsin as a prototype for proton pumps. *J. Biol. Chem.* 272:31209–31212.

Lazarova, T., C. Sanz, E. Querol, and E. Padrós. 2000. Fourier transform infrared evidence for early deprotonation of Asp^{85} at alkaline pH in the photocycle of bacteriorhodopsin mutants containing E194Q. *Biophys. J.* 78:2022–2030.

Luecke, H., H. T. Richter, and J. K. Lanyi. 1998. Proton transfer pathways in bacteriorhodopsin at 2.3 angstrom resolution. *Science.* 280:1934–1937.

Mathies, P. A., S. W. Lin, J. B. Ames, and W. T. Pollard. 1991. From femoseconds to biology: mechanism of bacteriorhodopsin's light-driven proton pump. *Annu. Rev. Biophys. Biophys. Chem.* 20:491–518.

Oesterhelt, D., and W. Stoeckenius. 1974. Isolation of the cell membrane of Halobacterium halobium and its fractionation into red and purple membrane. *Methods Enzymol.* 31:667–678.

Onishi, H., E. M. McCance, and N. E. Gibbons. 1965. A synthetic medium for extremely halophilic bacteria. *Can. J. Microbiol.* 11:365–373.

Ovchinnikov, Y. A. 1982. Rhodopsin and bacteriorhodopsin: structure-function relationships. *FEBS Lett.* 148:179–191.

Riesle, J., D. Oesterhelt, N. A. Dencher, and J. Heberle. 1996. D38 is an essential part of the proton translocation pathway in bacteriorhodopsin. *Biochemistry.* 35:6635–6643.

Rothwell, W. P., and J. S. Waugh. 1981. Transverse relaxation of dipolar coupled spin systems under rf irradiation: detecting motions in solid. *J. Chem. Phys.* 74:2721–2732.

Saitô, H. 1986. Conformation-dependent ^{13}C chemical shifts: a new means of conformational characterization as obtained by high-resolution solid-state NMR. *Magn. Reson. Chem.* 24:835–852.

Saitô, H., and I. Ando. 1989. High-resolution solid-state NMR studies of synthetic and biological macromolecules. *Annu. Rep. NMR Spectrosc.* 21:209–290.

Saitô, H., S. Tuzi, and A. Naito. 1998. Empirical versus nonempirical evaluation of secondary structure of fibrous and membrane protein by solid-state NMR: a practical approach. *Annu. Rep. NMR Spectrosc.* 36:79–121.

Saitô, H., S. Tuzi, S. Yamaguchi, M. Tanio, and A. Naito. 2000. Conformation and backbone dynamics of bacteriorhodopsin as revealed by ^{13}C NMR. *Biochim. Biophys. Acta.* 1460:39–48.

Saitô, H., S. Tuzi, M. Tanio, and A. Naito. 2002a. Dynamic aspect of membrane proteins and membrane-associated peptides as revealed by 13C NMR: lessons from bacteriorhodopsin as an intact protein. *Annu. Rep. NMR Spectrosc.* 47:39–108.

Saitô, H., T. Tsuchida, K. Ogawa, T. Arakawa, S. Yamaguchi, and S. Tuzi. 2002b. Residue-specific millisecond to microsecond fluctuations in bacteriorhodopsin induced by disrupted or disorganized two-dimensional crystalline lattice, through modified lipid-helix and helix-helix interactions, as revealed by ^{13}C NMR. *Biochim. Biophys. Acta.* 1565:97–106.

Saitô, H., R. Kawaminami, M. Tanio, T. Arakawa, S. Yamaguchi, and S. Tuzi. 2002c. Dynamic aspect of bacteriorhodopsin as viewed from ^{13}C NMR: conformational elucidation, surface dynamics and information transfer from the surface to inner residues. *Spectrosc. Int. J.* 16: 107–120.

Saitô, H., J. Mikami, S. Yamaguchi, M. Tanio, A. Kira, T. Arakawa, K. Yamamoto, and S. Tuzi. 2004. Site-directed ^{13}C solid-state NMR studies on membrane proteins: strategy and goals toward conformation and dynamics as illustrated for bacteriorhodopsin labeled with [1-^{13}C]amino-acid residues. *Magn. Reson. Chem.* 4:218–230.

Saitô, H., K. Yamamoto, S. Tuzi, and S. Yamaguchi. 2003. Backbone dynamics of membrane proteins in lipid bilayers: the effect of two dimensional array formation as revealed by site-directed solid-state ^{13}C NMR studies on [3-^{13}C]Ala- and [1-^{13}C]Val-labeled bacteriorhodopsin. *Biochim. Biophys. Acta* 1616:127–136.

Sanz, C., T. Lazarova, F. Sepulcre, R. González-Moreno, J.-L. Bourdelande, E. Querol, and E. Padrós. 1999. Opening the Schiff base moiety of bacteriorhodopsin by mutation of the four extracellular Glu side chains. *FEBS Lett.* 4556:191–195.

Sanz, C., M. Márquez, A. Perálvarez, S. Elouatik, F. Sepulcre, E. Querol, T. Lazarova, and E. Padrós. 2001. Contribution of extracellular Glu residues to the structure and function of bacteriorhodopsin. Presence of specific cation-binding sites. *J. Biol. Chem.* 276:40788–40794.

Solomon, I. 1955. Relaxation processes in a system of two spins. *Phys. Rev.* 99:559–565.

Stoeckenius, W., and R. A. Bogomolni. 1982. Bacteriorhodopsin and related pigments of halobacteria. *Annu. Rev. Biochem.* 52:587–616.

Suwelack, D., W. P. Rothwell, and J. S. Waugh. 1980. Slow molecular motion detected in the NMR spectra of rotating solids. *J. Chem. Phys.* 73:2559–2569.

Szundi, L., and W. Stoeckenius. 1987. Effect of lipid surface charges on the purple-to-blue transition of bacteriorhodopsin. *Proc. Natl. Acad. Sci. USA.* 84:3681–3684.

Szundi, L., and W. Stoeckenius. 1989. Surface pH controls purple-to-blue transition of bacteriorhodopsin. *Biophys. J.* 56:369–383.

Tanio, M., S. Tuzi, S. Yamaguchi, R. Kawaminami, A. Naito, R. Needleman, J. K. Lanyi, and H. Saitô. 1999. Conformational changes of bacteriorhodopsin along the proton-conduction chain as studied with ^{13}C NMR of [3-^{13}C]Ala-labeled protein: Arg82 may function as an information mediator. *Biophys. J.* 77:1577–1584.

Tuzi, S., J. Hasegawa, R. Kawaminami, A. Naito, and H. Saitô. 2001. Regio-selective detection of dynamic structure of membrane alpha-helices as revealed by ^{13}C NMR spectra of [3-^{13}C]Ala-labeled bacteriorhodopsin in the presence of Mn^{2+} ion. *Biophys. J.* 81:425–434.

Tuzi, S., A. Naito, and H. Saitô. 1993. A high-resolution solid-state ^{13}C NMR study on [1-^{13}C]Ala and [3-^{13}C]Ala and [1-^{13}C]Leu and Val-labelled bacteriorhodopsin. Conformation and dynamics of transmembrane helices, loop and termini, and hydration-induced conformational change. *Eur. J. Biochem.* 218:837–844.

Tuzi, S., A. Naito, and H. Saitô. 2003. Local protein structure and dynamics at kinked transmembrane α-helices of [1-^{13}C]Pro-labeled bacteriorhodopsin as revealed by site-directed ^{13}C NMR. *J. Mol. Struct.* 654:205–214.

Tuzi, S., S. Yamaguchi, A. Naito, R. Needleman, J. K. Lanyi, and H. Saitô. 1996. Conformation and dynamics of [3-^{13}C]Ala-labeled bacteriorhodopsin and bacterioopsin, induced by interaction with retinal and its analogs, as studied by ^{13}C nuclear magnetic resonance. *Biochemistry.* 35:7520–7527.

Tuzi, S., S. Yamaguchi, M. Tanio, H. Konishi, S. Inoue, A. Naito, R. Needleman, J. K. Lanyi, and H. Saitô. 1999. Location of cation-binding site in the loop between helices F and G of bacteriorhodopsin as studied by ^{13}C NMR. *Biophys. J.* 76:1523–1531.

Yamaguchi, S., S. Tuzi, M. Tanio, A. Naito, J. K. Lanyi, R. Needleman, and H. Saitô. 2000. Irreversible conformational change of bacterio-opsin induced by binding of retinal during its reconstitution to bacteriorhodopsin, as studied by ^{13}C NMR. *J. Biochem. (Tokyo).* 127:861–869.

Yamaguchi, S., S. Tuzi, K. Yonebayashi, A. Naito, R. Needleman, J. K. Lanyi, and H. Saito. 2001a. Surface dynamics of bacteriorhodopsin as revealed by ^{13}C NMR studies on ^{13}CAla-labeled proteins: detection of millisecond or microsecond motions in interhelical loops and C-terminal α-helix. *J. Biochem. (Tokyo).* 129:373–382.

Yamaguchi, S., K. Yonebayashi, H. Konishi, S. Tuzi, A. Naito, J. K. Lanyi, R. Needleman, and H. Saitô. 2001b. Cytoplasmic surface structure of bacteriorhodopsin consisting of interhelical loops and C-terminal α-helix, modified by a variety of environmental factors as studied by ^{13}C-NMR. *Eur. J. Biochem.* 268:2218–2228.

Yamazaki, Y., M. Hatanaka, H. Kandori, J. Sasaki, W. F. Karsten, J. Raap, J. Lugtenburg, M. Bizounok, J. Herzfeld, R. Needleman, and J. K. Lanyi. 1995. Interaction of tryptophan-182 with the retinal 9-methyl group in the L intermediate of bacteriorhodopsin. *Biochemistry.* 34:7088–7093.

Yamazaki, Y., S. Tuzi, H. Saitô, H. Kandori, R. Needleman, J. K. Lanyi, and A. Maeda. 1996. Water structural changes at the proton uptake site (the Thr46-Asp96 domain) in the L-intermediate of bacteriorhodopsin. *Biochemistry.* 35:4063–4068.

Yonebayashi, K., S. Yamaguchi, S. Tuzi, and H. Saitô. 2003. Cytoplasmic surface structures of bacteriorhodopsin modified by site-directed mutations and cation binding as revealed by ^{13}C NMR. *Eur. Biophys. J.* 32:1–11.